

Free volume under shear

Moumita Maiti,¹ H. A. Vinutha,^{2,3} Srikanth Sastry,^{2,3} and Claus Heussinger¹

¹*Institute for Theoretical Physics, Georg-August University of Göttingen,
Friedrich-Hund Platz 1, 37077 Göttingen, Germany*

²*Jawaharlal Nehru Center for Advanced Scientific Research,
Jakkur Campus, Bengaluru – 560064, India*

³*TIFR Center for Interdisciplinary Sciences,
21 Brundavan Colony, Narsingi, 500075 Hyderabad, India*

(Dated: June 23, 2015)

Abstract

Using an athermal quasistatic simulation protocol, we study the distribution of free volumes in sheared hard-particle packings close to, but below, the random-close packing threshold. We show that under shear, and independent of volume fraction, the free volumes develop features similar to close-packed systems – particles self-organize in a manner as to mimick the isotropically jammed state. We compare athermally sheared packings with thermalized packings and show that thermalization leads to an erasure of these structural features. The temporal evolution, in particular the opening-up and the closing of free-volume patches is associated with the single-particle dynamics, showing a crossover from ballistic to diffusive behavior.

I. INTRODUCTION

The transition from a flowing liquid to a jammed solid state has been a subject of research in a wide range of systems, including granular matter, colloidal suspensions, and diverse types of glass formers, and in the context of gelation. A particular context, in which the geometry associated with such a transition is important, has been that of the jamming to unjamming transition in athermal particle packings, often modeled using sphere packings, with or without the presence of external driving. The relationship between the jamming phenomenology and thermal systems, either the rheology of driven thermal systems, or to the glass transition in undriven systems, are intensely investigated currently [1–3].

Disordered assemblies of spheres undergo a *jamming* transition at a packing fraction of ~ 0.64 , at which the pressure for hard sphere packings diverges. At this *random close packing* (RCP) density, individual hard spheres are entirely constrained by their neighbours and have no space to move around. The network of such spheres in contact (“backbone”) spans the system and may thus support external load.

The geometrical properties of sphere packings and their influence on the mechanical response is a complex problem with many different facets. One key observable is the connectivity of the network which is isostatic at RCP [4–6]. Wyart [8] discussed the consequences of opening of contacts, as well as the distribution of gaps, i.e. distances between non-contacting particles. Atkinson et al. [9] have studied the structure of rattlers, the particles that are not constrained by enough contacts. Schröder-Turk et al. [10] have observed a signature of RCP in the shape of Voronoi cells of the particles.

Packings at RCP also have special mechanical properties. The bulk modulus, for example, is finite for soft-sphere packings at RCP, while it generically vanishes for spring networks of equivalent connectivity [11, 12]. Apparently, the particles in a packing can *organize* in order to resist compressive forces, in a way that is not possible for spring networks.

In the vicinity of random close packing, spheres have finite free space to move, and free space vanishes approaching RCP. For thermal systems this implies slow dynamics approaching RCP. At the same time, dynamics in sheared systems at zero temperature speeds up by approaching RCP. Indeed, particles in shear flow are found to move ever faster, the less space they have [13]. It is an interesting but essentially unsolved question how such non-trivial dynamics arises and couples to other properties of the system, in particular to

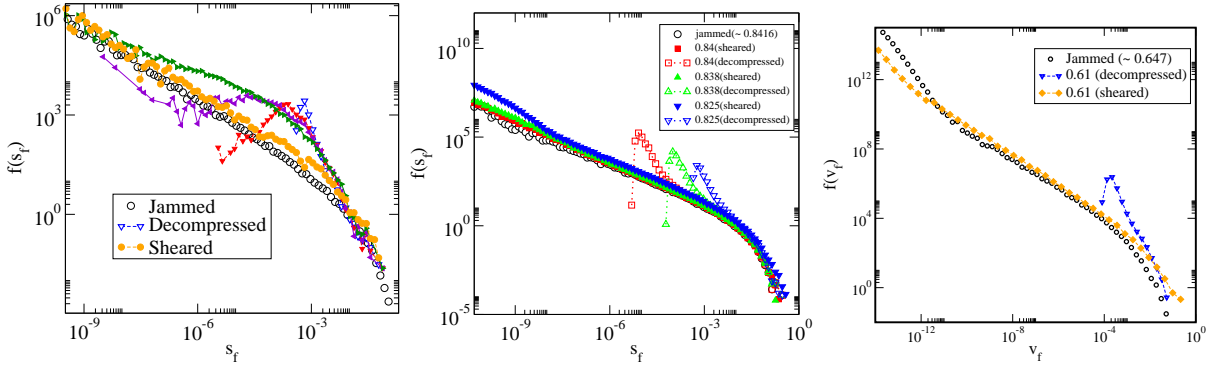


FIG. 1: Probability distribution of free volumes (2D): (a) $\phi = 0.825$ for decompressed (unsheared) configurations and for different elapsed strains; (b) Different volume fractions in the steady state and compared with the distribution for nearly jammed configurations. (c) Data for the 3D system.

the singular behavior of the correlation length or the rheological coefficients [14–18]. Here, we are interested in the analysis of the free space available for particle movement, and how that may be affected by externally imposed deformation, and in turn how such changes in geometry influence particle flow.

The divergence of pressure in a hard particle system is a consequence of the vanishing of free space. Pressure is the ratio of free surface to free volume [7], the latter vanishes at jamming. In the fluid phase, the free volume distribution is peaked around the mean free volume, and at jamming the distribution can be expected to have a delta function peak at zero free volume for the backbone spheres. Indeed close to jamming, for isotropic, thermalized, ensembles of configurations at any given density, the free volume distribution [19] has a strong peak around the mean free volume. A surprising observation, however, is that there is a power law tail in the free volume distribution in addition, which appears to be a signature of being close to the jamming point. In the present work, we address the question of how the free volume distributions of sphere packings close to the jamming point get modified under shear deformation, both in the athermal and thermal cases, and what we may deduce regarding the organization of spheres in response to external shear.

II. SIMULATION DETAILS

We study two- (2D) and three-dimensional (3D) systems of N soft frictionless spheres. To avoid crystallization, we use two different particle sizes; $\frac{N}{2}$ spheres have diameter d and

$\frac{N}{2}$ have diameter $1.4d$. The particle density is quantified via the fraction of volume (area in 2D, although we use ‘volume’ in the 2D case as well, when no confusion is caused) ϕ that is occupied by the particles.

Particles interact via elastic repulsive forces. Two particles repel each other with a harmonic potential energy,

$$E_{\text{el}} = -\epsilon \left(1 - \frac{r_{ij}}{d_{ij}}\right)^2, \quad r_{ij} < d_{ij} \quad (1)$$

where r_{ij} is the distance between the two particles. The cut-off $d_{ij} = (d_i + d_j)/2$ is set by the diameters of the two interacting spheres.

To implement the shear a quasistatic simulation protocol is used [21, 22]. In the quasistatic limit (small-strain rates, $\dot{\gamma} \rightarrow 0$) the average overlap $\delta = \langle 1 - \frac{r_{ij}}{d_{ij}} \rangle$, vanishes and the particles effectively behave as hard-spheres (equivalent to $\epsilon \rightarrow \infty$). In recent work [18, 20] it was shown that the statistics of particle velocities obtained from the quasi-static simulations is identical with the small-strain rate (Newtonian fluid) limit of fully dynamic molecular dynamics simulations. Thus, our quasistatic results should be considered representative for the Newtonian flow-regime of dense suspensions close to jamming.

The jamming density under shear is at $\phi_c = 0.647$ ($\phi_c = 0.842$ in 2D). We probe densities below this limit in the range $\phi = 0.61 - 0.64$ ($\phi = 0.825 \dots 0.840$ in 2d). In this range of densities cooperative effects set in and the correlation length increases roughly by a factor of ten [13].

III. RESULTS

Motivated by recent results on the free volume distribution in isotropically jammed packings [19], we ask how steady shear affects these distributions. The free volume of a particle is the volume (area in 2D) that is available for the center of the particle with all other particles are fixed in space.

Starting with a jammed configuration at ϕ_c , we decompress the configuration to the target density at $\phi < \phi_c$ by reducing the diameters of all particles, $d_i \rightarrow \alpha d_i$, where α is the scaling factor for the particle diameters. In this way, all particles acquire a certain amount of free volume v_f (or free surface s_f in the two dimensional case) with a probability distribution, $P(v_f)$, that is highly peaked at $v_f \sim \alpha^d$ (see Fig. 1 (a) for the 2d system, blue

line/downward triangles). In this figure we also highlight the distribution of free volume for the nearly jammed configuration (before decompression), which is a power-law (black open circles) [19].

The “decompressed” configuration serves as starting point to our shear simulation. Fig. 1 (a) indicates the evolution of the probability distribution as a function of the elapsed strain. After only small amounts of strain, all particles retain their finite free volume, but as straining goes on the number of those particles reduce and a peak at zero free volume starts developing (not shown in the figure). At the same time, a broad tail develops. In the steady-state, thus, the form of the distribution is rather different than in the decompressed configuration. Instead of a narrow, peaked distribution we obtain a strong peak at zero free volume with a broad power law tail.

Fig. 1 (b) illustrates that, close to jamming, the power-law tail is independent of density ϕ , which is also identical in the exponent to the isotropically jammed state. The same phenomenon is observed also for the three-dimensional system, as shown in Fig. 1 (c), illustrating that the outcome is not dependent on dimensionality. Apparently, during shear particles self-organize in such a way as to mimick the isotropically jammed state – even though the system is not jammed and flows as a Newtonian liquid.

It is worthwhile comparing the situation of steady shear with that of cyclic shear. Experiments performed at low densities [24, 25] have shown that after sufficient shear cycles the system self-organizes into an “absorbing” state, where particles do not interact anymore. Their trajectories during a shear cycle are strictly reversible. This indicates that particles generate free volume around themselves in such a way that during their shear-induced oscillations no interactions with other particles occur. Under steady-shear the organization apparently is opposite, and free volume is not generated but destroyed (Fig. 2). The average free volume under shear is roughly two orders of magnitude smaller compared to the decompressed configuration at the same density.

Another illustrative comparison is with thermal systems. Recall that the system we study is inherently athermal. Particles only move because they are driven by shear. To generate a thermalized system at the same density we again use the decompressed state as starting configuration, but now run short Metropolis Monte-Carlo simulations. The resulting free volume distribution is presented in Fig. 3 and compared to the sheared state.

It is clear that thermalization acts rather differently than shearing and does not produce

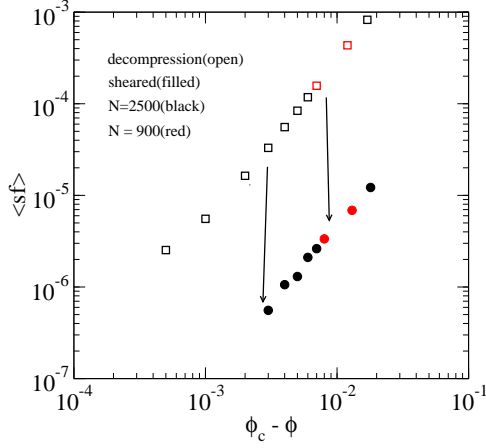


FIG. 2: Average free volume as a function of volume fraction. Comparison of configurations under shear and decompressed states. Two different system sizes are compared to exclude finite-size effects.

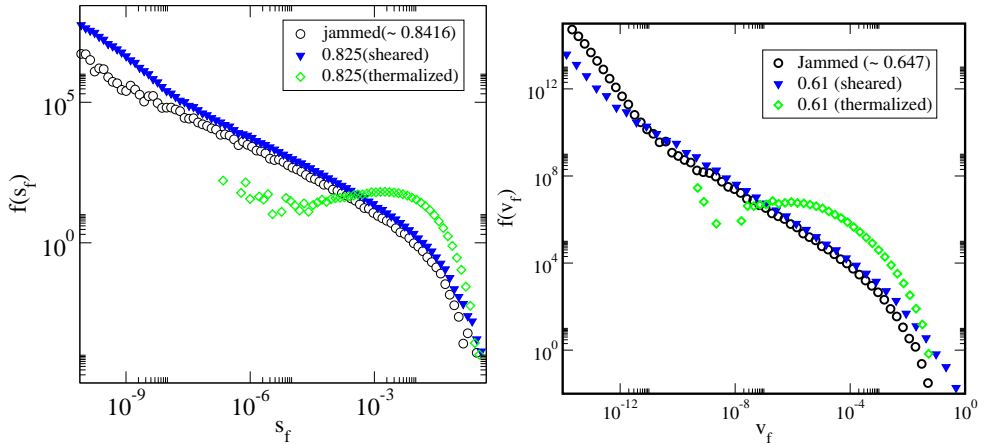


FIG. 3: Comparison of free-volume distributions from jammed, sheared and thermalized configurations (top: 2D, bottom: 3D).

a power-law tail in the free volume distribution (in agreement with Ref. [19]). This is interesting also from the point of view of shear-induced effective temperatures [26–29], which rely on the assumption that driving by shear is in some sense equivalent to thermal driving but at an “effective” temperature. At least for the observable under consideration – the free-volume distribution – this equivalence does not seem to hold here.

Another difference between the sheared and thermal systems is the distribution of the total free volume among the particles. In the thermal system (and also under cyclic shear) the free volume is distributed basically among all particles. In the sheared system, only a

certain fraction of particles have a non-zero free volume. In the density range we studied, we find a fraction of 6% to 11% of such finite free volume particles. The majority of particles belong to a backbone of locally jammed particles with zero free volume. The full free-volume distribution therefore consists of a power-law tail for particles with finite free volume plus a delta-function peak for the backbone particles. As the density is increased, more and more finite free volume particles are incorporated into the backbone, such that at ϕ_c the backbone becomes globally jammed and the system solidifies.

A structural self-organization via shear flow is also visible in the pair-correlation function. The power law singularity as well as the splitting of the second peak are commonly taken as the signature of the jammed state. Fig. 4 shows that sheared configurations exhibit a similar power-law singularity with the same exponent as in the jammed state, whereas thermalization destroys the divergence. Also the splitting of the second peak in steady-shear is as sharp as in the jammed state but it is smeared out under thermalization. We have also computed the radial distribution function only for the finite free volume particles and find it to be similar as for particles with zero free volume. This is consistent with the findings of Atkinson *et al.* [9] who report a certain amount of spatial correlations in the rattlers.

Solidification is known to occur when the backbone is exactly isostatic. We can extract the approach to isostaticity also from the free volumes. To this end we shrink the particles (in the steady-state shear configurations) by a very small factor f . This generates a finite free volume $v = \mathcal{O}(f^d)$ for the backbone particles. The average number of facets of these free volume patches then defines the connectivity of the backbone.

Fig. 5 shows that the backbone network is hypostatic (as expected in the fluid regime below jamming) and thus not mechanically stable. Isostaticity is approached as $z_{\text{iso}} - z \sim (\phi_c - \phi)^x$, with an exponent x close to one. Being hypostatic, there are a number of zero frequency modes along which particles can move without cost in energy. This motion is, for example, visible as a short-time ballistic regime in the mean-square displacement [13]. Similarly, this motion is reflected in the temporal evolution of the free volume of the finite free volume particles. The locations of such particles represent holes in the network of backbone particles and how these holes close or open-up reflects how particles move in the network.

We calculate the strain needed to close a hole. This represents a measure for the “life-

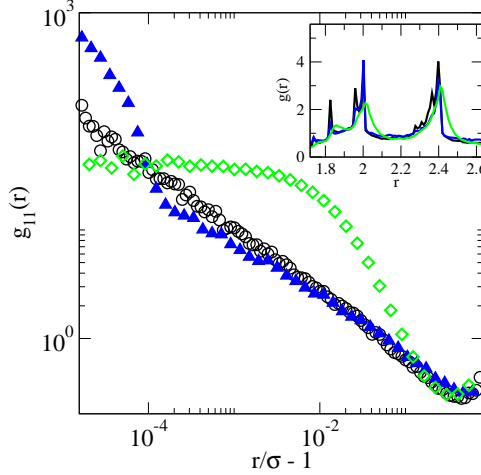


FIG. 4: Pair correlation function $g(r)$ for jammed packing, as well as sheared and thermalized configurations (color code as in Fig. 3). Sheared configurations display the same characteristic power-law slope as the jammed configuration. Thermalization destroys this power-law. Inset shows that sheared configurations have a split-second peak as seen in jammed configurations, whereas for thermalized configurations, the sharp features are smeared out.

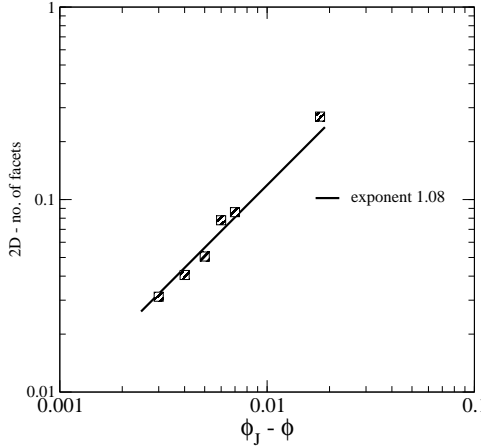


FIG. 5: Effective connectivity in the backbone of zero-free volume particles – measured via the number of facets of the free volume after tiny amount of decompression.

time” of finite free volume for a particle that resides in this hole. The probability distribution of strains to close the holes is displayed in Fig. 6. The striking feature is its power-law tail, which is a consequence of the broad distribution of hole sizes. Holes can close after arbitrarily small strains. On large strain-scales, the tail is cut-off at strains γ_c that decrease with increasing the volume-fraction towards ϕ_c . In fact, the cut-off γ_c is comparable in

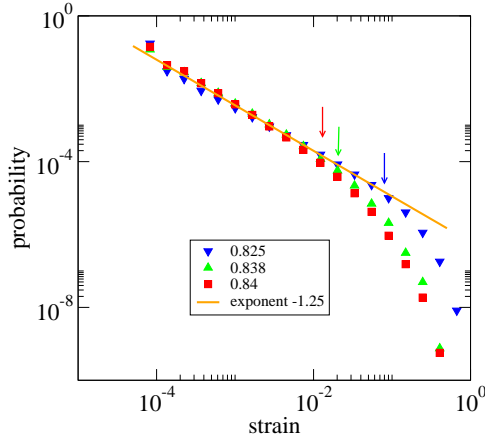


FIG. 6: The distribution of strain values needed for closing a hole. The arrows signify the strain γ_{msd} , at which the particle dynamics (as measured by the mean-square displacement, msd) crosses over from ballistic to diffusive (taken from Ref.[13]).

magnitude to the strain γ_{msd} , at which the mean-squared displacement has a crossover from ballistic to diffusive behavior (extracted from Fig. 1 in Ref. [13]). The strains γ_{msd} for three different ϕ are indicated in Fig. 6 by arrows. This connects the evolution of free-volume patches – holes in the network of backbone particles – with the single-particle dynamics. The cross-over to diffusion signals the onset of the decorrelation of the floppy, zero-energy modes, and this decorrelation is associated by the opening and closing of these holes.

IV. CONCLUSION

In conclusion, we have shown that *unjammed athermal hard-particle systems under shear* self-organize such that structural properties resemble those of *jammed packings*. In particular, we have reported the probability distribution of free-volumes as well as the pair-correlation function.

The free-volume distribution in (nearly-)jammed packings has previously been shown to display a power-law tail [19]. We show here that this tail is also present in sheared systems in a finite interval of densities below the jamming threshold. By way of contrast, thermalized configurations in this density range generically show a peaked and rather narrow distribution of free volumes.

Apparently, shearing and thermalization act rather differently what regards these lo-

cal structural properties. Shearing drives the system “towards” the jamming point, while thermalization drives the system away from it.

The average free volume in the sheared configurations is roughly two orders of magnitude smaller than in the thermalized configurations. Moreover free volume is heterogeneously distributed among only a few finite free volume particles, with the majority of particles belonging to a locally jammed backbone with zero free volume.

Our results raise the question about the relevance of finite free volume particles for the flow properties close to jamming. Indeed, a power-law in the free-volume distribution means that there are particles with arbitrarily-small amounts of extra space. As a consequence, they can easily be integrated into the backbone after only infinitesimal amounts of strain.

Acknowledgments

We acknowledge financial support by the German Science Foundation via the Emmy Noether program (He 6322/1-1).

- [1] A. J. Liu and S. R. Nagel, *Nature* **396**, 21 (1998).
- [2] A. J. Liu and S. R. Nagel, *Annu. Rev. Condens. Matter Phys.* **1** 347-369 (2010).
- [3] S. Torquato and F.H. Stillinger, *Rev. Mod. Phys.* **82**, 2633 (2010).
- [4] C. F. Moukarzel Phys. Rev. Lett. **81**, 1634 (1998).
- [5] C. S. OHern, L. E. Silbert, A. J. Liu, S. R. Nagel, Phys. Rev. E **68** 011306 (2003).
- [6] M. Wyart, Ann. Phys. (France) **30** 1 (2005).
- [7] R. J. Speedy, J. Chem. Soc. Faraday Trans II **76**, 693 (1980).
- [8] M. Wyart, Phys. Rev. Lett. **109**, 125502 (2012), URL <http://link.aps.org/doi/10.1103/PhysRevLett.109.125502>.
- [9] S. Atkinson, F. H. Stilinger, and S. Torquato, Phys. Rev. E **88**, 062208 (2013).
- [10] G. E. Schröder-Turk, W. Mickel, M. Schröter, G. W. Delaney, M. Saadatfar, T. J. Senden, K. Mecke, and T. Aste, Europhys. Lett. **90**, 34001 (2010).
- [11] W. G. Ellenbroek, Z. Zeravcic, W. van Saarloos, and M. van Hecke, Europhys. Lett. **87**, 34004 (2009).

[12] M. Sheinman, C. P. Broedersz, and F. C. MacKintosh, Phys. Rev. E **85**, 021801 (2012), URL <http://link.aps.org/doi/10.1103/PhysRevE.85.021801>.

[13] C. Heussinger,, L. Berthier,, and J.-L. Barrat,, EPL **90**, 20005 (2010), URL <http://dx.doi.org/10.1209/0295-5075/90/20005>.

[14] P. Olsson and S. Teitel, Phys. Rev. Lett. **109**, 108001 (2012), URL <http://link.aps.org/doi/10.1103/PhysRevLett.109.108001>.

[15] B. P. Tighe, Phys. Rev. Lett. **107**, 158303 (2011), URL <http://link.aps.org/doi/10.1103/PhysRevLett.107.158303>.

[16] M. Otsuki and H. Hayakawa, Physical Review E (Statistical, Nonlinear, and Soft Matter Physics) **80**, 011308 (pages 12) (2009).

[17] E. Lerner, G. Düring, and M. Wyart, Proc. Natl. Acad. Sci. USA **109**, 4798 (2012), URL <http://www.pnas.org/content/109/13/4798.full.pdf+html>, URL <http://www.pnas.org/content/109/13/4798.abstract>.

[18] B. Andreotti, J.-L. Barrat, and C. Heussinger, Phys. Rev. Lett. **109**, 105901 (2012), URL <http://link.aps.org/doi/10.1103/PhysRevLett.109.105901>.

[19] M. Maiti and S. Sastry, The Journal of Chemical Physics **141**, 044510 (2014).

[20] M. Maiti and C. Heussinger, Phys. Rev. E **89**, 052308 (2014).

[21] C. Heussinger and J.-L. Barrat, Phys. Rev. Lett. **102**, 218303 (2009).

[22] C. Heussinger, P. Chaudhuri, and J.-L. Barrat, Soft Matter **6**, 3050 (2010).

[23] C. S. O’Hern, S. A. Langer, A. J. Liu, and S. R. Nagel, Phys. Rev. Lett. **88**, 075507 (2002).

[24] D. J. Pine, J. P. Gollub, J. F. Brady, and A. M. Leshansky, Nature **438**, 997 (2005).

[25] L. Corte, P. M. Chaikin, J. P. Gollub, and D. J. Pine, Nature Phys. **4**, 420 (2008).

[26] T. K. Haxton, and A. J. Liu, Phys. Rev. Lett. **99**, 195701 (2007).

[27] L. Berthier and J.-L. Barrat, *J. Chem. Phys.* **116**, 6228 (2002).

[28] E. Bouchbinder, J. S. Langer and I. Procaccia, *Phys. Rev. E* **75**, 036107 (2007).

[29] I. K. Ono, C. O’Hern, D. J. Durian, S. A. Langer, A. J. Liu and S. R. Nagel, *Phys. Rev. Lett.* **89**, 095703 (2002).